THE JOURNAL OF BIOLOGICAL CHEMISTRY Vol. 280, No. 12, Issue of March 25, pp. 11379–11386, 2005
Printed in U.S.A.

Phosphoinositide 3-Kinase Is Required for Intracellular *Listeria monocytogenes* Actin-based Motility and Filopod Formation*[S]♦

Received for publication, December 23, 2004
Published, JBC Papers in Press, January 10, 2005, DOI 10.1074/jbc.M414533200

Gurjit Sidhu‡, Wei Li‡, Nicholas Laryngakis‡, Ellen Bishai‡, Tamas Balla§, and Frederick Southwick‡¶

From the ‡Department of Medicine, Division of Infectious Diseases, University of Florida College of Medicine, Gainesville, Florida 32610 and the §Endocrinology and Reproduction Research Branch, NICHD, National Institutes of Health, Bethesda, Maryland 20982-4510

Motile nonmuscle cells concentrate phosphatidylinositol 3,4,5-trisphosphate (PtdIns(3,4,5)P_3) and phosphatidylinositol 4,5-bisphosphate (PtdIns(4,5)P_2) in areas of new actin filament assembly. There is great interest in assessing the *in vivo* functional significance of these phosphoinositides, and we have used *Listeria monocytogenes* to explore the contribution of PtdIns(3,4,5)P_3 and PtdIns(4,5)P_2 to its actin-based motility. In *Listeria*-infected PtK2 cells Akt-pleckstrin homology (PH)-green fluorescent protein (GFP) and phospholipase Cδ (PLCδ)-PH-GFP both first concentrate at the front of motile *Listeria*, subsequently surrounding the bacterium and then concentrating in the actin filament tail. Surprisingly, *Listeria* ActA mutant strains lacking the putative phosphoinositide binding site are also able to concentrate these probes. Reduction of available PtdIns(3,4,5)P_3 by expression of Akt-PH-GFP and available PtdIns(4,5)P_2 by expression of PLCδ-PH-GFP both significantly slow *Listeria* actin-based movement. Treatment of cells with the PI 3-kinase inhibitor, LY294002, dissociates Akt-PH but not PLCδ-PH, from the bacterial surface and cell membranes, and results in near complete inhibition of *Listeria* actin-based motility and filopod formation. Removal of LY294002 results in rapid and full recovery of Akt-PH localization, *Listeria* actin-based motility, and filopod formation. These findings suggest that PtdIns(4,5)P_2 is concentrated at the surface of *Listeria* and serves as the substrate for PtdIns(3,4,5)P_3 production, indicating a central role for PI 3-kinases in *Listeria* intracellular actin-based motility and filopod formation.

The onset of actin-based cell motility in nonmuscle cells is signaled by the increased turnover of phosphoinositides, and phosphoinositides are known to interact with and regulate multiple actin-binding proteins, kinases, and guanine nucleotide exchange factors (1, 2). Following exposure to various agonists that stimulate cell migration, plasma membrane PtdIns(4,5)P_2[1] is converted to PtdIns(3,4,5)P_3, which is then concentrated at the leading edge of the cell membrane. The accumulation of PtdIns(3,4,5)P_3 at these sites is associated with the formation of new actin filaments (3). The mechanisms by which these lipid products induce actin assembly are under active investigation and include the uncapping of actin filaments and stimulation of actin nucleation (2).

The shape changes associated with chemotaxis, cell spreading, and phagocytosis are complex and make analysis of rates and directionality of actin assembly difficult. Furthermore, these events involve several steps of receptor-mediated signal transduction. *Listeria* intracellular infection and movement is a particularly useful model for examining the parameters of *in vivo* actin assembly, allowing discrete temporal and spatial resolution of actin filament formation. Intracellular *Listeria* infection of tissue culture cells is accomplished by simply overlaying the bacteria on the surface of host cells. Internalins found on the surface of the bacterium bind to host cell receptors that induce phagocytosis (4). Once ingested, the bacterium escapes from the phagolysosome by lysing the confining membrane (5) and then rapidly multiplies within the cytoplasm. Within 2–3 h, the bacterium induces actin assembly at one pole, forming a discrete polymerization zone where new actin monomers are added to the growing filaments (6, 7). Actin filament assembly provides directional force that drives the bacterium through the cytoplasm to the peripheral membrane of the cell. Here the bacterium pushes the membrane outward forming a discrete filopod that can be ingested by an adjacent cell, and the cycle is repeated. The bacterial surface protein ActA directly stimulates actin assembly, bypassing the receptor-mediated signal transduction pathways that induce actin filament formation during phagocytosis and chemotaxis (8). Curiously, ActA has a phosphoinositide binding site in the amino-terminal region that is located within amino acids 184–202 (9, 10), and binding of PtdIns(4,5)P_2 and PtdIns(3,4,5)P_3 causes a conformational change in the amino terminus of ActA. However, *in vivo* phosphoinositide localization studies have not been performed, and the physiological significance of the inositide binding site has not been examined. In the present study we used green fluorescent protein chimeras linked to the pleckstrin homology (PH) domains of phospholipase C (PLCδ) (11) and of Akt (protein kinase B) (12), which bind PtdIns(4,5)P_2 and PtdIns(3,4,5)P_3 or PtdIns(3,4)P_2, respectively, to investigate the involvement of these phosphoinositides in *Listeria* motility. We show that both wild type *Listeria* and *Listeria* strains expressing an ActA mutant lacking the putative phosphoinositide binding site are capable of concen-

* This work was supported by National Institutes of Health Grants RO1AI34276 and RO1AI-23262. The costs of publication of this article were defrayed in part by the payment of page charges. This article must therefore be hereby marked "*advertisement*" in accordance with 18 U.S.C. Section 1734 solely to indicate this fact.

♦ This article was selected as a Paper of the Week.

[S] The on-line version of this article (available at http://www.jbc.org) contains a supplemental video.

¶ To whom correspondence should be addressed: Division of Infectious Diseases, Box 100277, University of Florida College of Medicine, Gainesville, FL 32610. Tel.: 352-392-4058; Fax: 352-392-6481; E-mail: southfs@med.mac.ufl.edu.

[1] The abbreviations used are: PtdIns(4,5)P_2, phosphatidylinositol 4,5-bisphosphate; PtdIns(3,4,5)P_3, phosphatidylinositol 3,4,5-trisphosphate; PI 3-kinase, phosphoinositide 3-kinase; PH, pleckstrin homology; PLC, phospholipase C; MDCK, Madin-Darby canine kidney; GFP, green fluorescent protein; RFP, red fluorescent protein.

trating both of these probes on their surface and in the actin tails. Additionally, we have found that treatments that lower PtdIns(3,4,5)P_3 production or availability significantly inhibited *Listeria*-induced actin assembly. Most exciting was the finding that the PI 3-kinase inhibitor, LY294002, blocked the translocation of Akt-PH-GFP to the bacteria and profoundly inhibited *Listeria* actin-based motility and filopod formation. These effects were completely reversed by removal of the inhibitor. These experiments, for the first time, point to a central role for PI 3-kinase(s) and PtdIns(3,4,5)P_3 in *Listeria* actin-based motility.

EXPERIMENTAL PROCEDURES

Tissue Culture Methods and Infection Procedures—The PtK2 cells (derived from the kidney epithelium of the kangaroo rat *Potorous tridactylis*) or MDCK cells were seeded at a concentration of 1×10^6 cells per coverslip in 35-mm culture dishes in 3 ml of culture media (minimum Eagle's medium with 10% fetal calf serum, 1% penicillin-streptomycin) and incubated for 48 h at 37 °C and 5% CO_2. Cells were infected as described previously (6) with minor modifications. Briefly *Listeria monocytogenes* strain was inoculated into brain heart infusion (Difco) and grown overnight at 37 °C, washed twice with Hanks' balanced salt solution (Life Technologies, Inc.) and then resuspended in minimum Eagle's medium without antibiotics to give a final concentration of 1×10^7 or a ratio of 10 bacteria per host cell. Bacteria in 2 ml of culture media were added to each dish followed by centrifugation at $400 \times g$ at room temperature for 10 min and then incubation for 45 min at 37 °C and 5% CO_2. After incubation, extracellular bacteria were removed by washing three times with Hanks' balanced salt solution. The culture media containing gentamicin sulfate (10 μg/ml) was added back to prevent extracellular growth of bacteria. The monolayer was then incubated for 1–5 h, and during this time video microscopy was performed. *Listeria* strains used in our experiments included 10403S and DP-L3982 (12) (missing ActA amino acids 171–235, Cossart amino acid nomenclature, kindly provided by Dr. Dan Portnoy, University of California, Berkeley), LO28 ActA-$\Delta_{158-231}$, and LO28 ΔActA with a wild type ActA plasmid (both kindly provided by Dr. Pascale Cossart, Institute Pasteur, Paris). The later two strains were grown in the presence of chloramphenicol as described previously (10). PtK2 cells were also infected with *Shigella flexneri* wild-type strain 2457T as described previously (13).

Transfection of Cells and Treatment with Inhibitors—Plasmids encoding the PH domains fused to the NH_2 terminus of green fluorescent protein or the monomeric red fluorescent protein were constructed as described previously (14). The plasmid constructs used included the PH domains of PLCδ-(1–170) or its mutant (R40L) and of the Akt protein kinase-(1–167) or its mutant (R25C). Plasmid DNAs (final concentration 2 μg/ml) were transfected into PtK2 or MDCK cells using the Lipofectamine reagent (10 μg/ml, Life Technologies, Inc.) as described previously (14). Cells were transfected 48 h prior to infection with *Listeria*.

For kinase inhibition experiments, standard protocols were utilized for treatment with wortmannin (final concentration 100 nM), LY294002 (final concentration 50 μM), and quercetin (final concentration 50 μM) (all obtained from Sigma). These inhibitors were added to infected cells 1–3 h after the initiation of infection, and bacterial velocities were measured before and 30–180 min after addition. For rat brain extract experiments, extract was prepared as described previously (15), and LY294002 was added simultaneously with the *Listeria* strain LO28 ΔActA containing a wild type ActA plasmid (see above). To depolymerize actin filaments Latrunculin A (Molecular Probes, Eugene, OR) (final concentration of 2 μM) was added to *Listeria*-infected PtK2 cells.

Microscopy—A Nikon Diaphot inverted microscope was equipped with a charge-coupled device camera (Hamamatsu), and the microscope stage temperature was maintained at 25 or 37 °C with a MS-200D perfusion microincubation system (Narishige, Tokyo). Images were also obtained using a MRC-1024 ES confocal microscope (Bio-Rad) sectioning at 0.2-μm intervals. Digital images were obtained and processed using the Metamorph image analysis program (Universal Imaging, West Chester, PA). Velocities of bacterial movement were determined by comparing the images at two time points and measuring the distance traveled by each bacterium using track points function (Metamorph program, Universal Imaging). Distances were calibrated using a Nikon micrometer. Differences in migration velocities were analyzed using the unpaired Student's *t* test or the Mann-Whitney nonparametric test. In each experiment the velocity of each moving bacterium was measured over 2 min giving 3 velocity measurements/bacteria. In all experiments *n* indicates the number of velocity measurements. We have previously noted marked variations in the velocity of actin-based motility in different tissue culture cell preparations. These differences probably relate to the age of the cells, the duration of adherence to glass coverslips, and possibly the growth conditions of the *Listeria*. Therefore to control for these variables each comparison of the velocities between transfected and control cells were made on the same tissue culture dish. In our kinase inhibitor experiments, cell preparations were split at the same time, and the same overnight culture of *Listeria* was used to infect all tissue culture plates.

Filamentous actin was stained using rhodamine-phalloidin as described previously (6). The relative intensity of 6×6 pixel regions of *Listeria* actin filament tails were measured using the regions statistics tool (Metamorph, Universal Imaging). Intracellular bacteria as compared with extracellular bacteria could be readily differentiated on time-lapse phase microscopy using two criteria. The refractive index of intracellular bacteria was distinctly different from extracellular bacteria. To confirm this observation, simultaneous phase and rhodamine-phalloidin images were compared. In analysis of 100 bacteria from 10 different cells, phase imaging demonstrated a 95% concordance with phalloidin staining in control cells. Secondly, on time-lapse video extracellular bacteria attached to the cell surface tended to twist and abruptly move in response to fluid currents whereas intracellular bacteria remained stationary or moved with relatively linear trajectories and constant velocities.

RESULTS

Localization of Akt-PH and PLCδ-PH in Listeria-infected Cells—Cells transfected with Akt-PH-GFP and PLCδ-PH-GFP took up bacteria and supported intracellular *Listeria* actin-based motility. During phagocytosis of the bacteria both GFP probes concentrated at the region of phagocytosis as observed previously in macrophages (16). As shown in Fig. 1*B*, Akt-PH-GFP concentrated around the ingested bacterium in the regions that were in direct contact with the plasma membrane. Once the bacteria were completely incorporated into the cell, the majority of intracellular bacteria was no longer associated with detectable fluorescence, the probe usually dissociating from the bacterial surface within 1–5 min. PLCδ-PH-GFP transfected cells demonstrated an identical pattern of localization during phagocytosis (Fig. 1*C*).

Subsequently, 3–4 h after the initiation of infection, bacteria again began attracting the two PH fluorescent probes. Simultaneous phase and fluorescence images revealed that a significant percentage of *Listeria* moving within the cell attracted PLCδ-PH-GFP to their actin filament tails and to the surface of the bacteria (Fig. 2). Time-lapse video (Fig. 2 video supplement) demonstrated that PLCδ-PH-GFP was first attracted to the front of the moving bacteria (example, Fig. 2, *A* and *B*, *arrowhead*). As the bacterium moved forward, the probe concentrated along the entire surface of the bacterium, as well as in the actin-rich tail (Fig. 2, *A* and *B*, *arrows*). Analysis of a number of moving bacteria showed that bacteria with distinct phase dense actin filament tails were more likely to concentrate PLCδ-PH-GFP (examples shown by the *arrows* in Fig. 2 and Fig. 2 video supplement). The percentage of motile bacteria concentrating the probe varied from 10 to 60%. Three-dimensional reconstruction of confocal images of PLCδ-PH-GFP transfected PtK2 cells revealed that motile bacteria concentrating the probe were consistently found within 0.6 μm of cell membrane. Once the bacteria began pushing out the peripheral membrane and forming filopodia all bacteria were surrounded by the PLCδ-PH probe (Fig. 2*C* and Fig. 2 video supplement). Rarely stationary bacteria were also surrounded by fluorescence; however, the majority of stationary intracellular bacteria could not be seen by fluorescence microscopy, only being seen by phase contrast imaging (compare *A* and *B* in Fig. 2).

Identical experiments were performed with cells transfected with Akt-PH-GFP, and this probe also localized to the bacterium and the actin-rich tails as *Listeria* moved through the

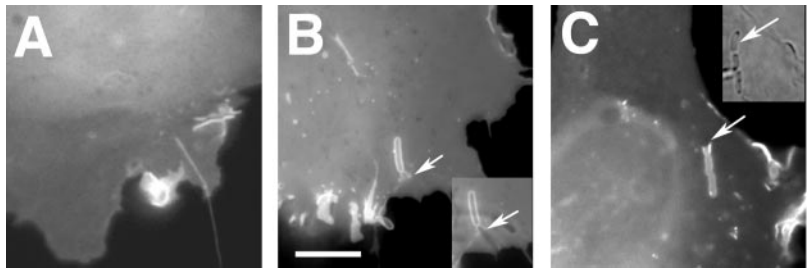

FIG. 1. **Localization of Akt-PH-GFP and PLCδ-PH-GFP during entry of *Listeria* monocytogenes into PtK2 cells.** Fluorescence images of PtK2 cells transfected with the PH-GFP constructs 24 h before infection with *Listeria*. *A*, time 0, prior to infection showing the Akt-PH domain localizing in active membrane ruffles. *B*, time 20–40 min after addition of *Listeria* to a culture dish containing cells transfected with Akt-PH-GFP. Two bacteria are being incorporated into the host cell by phagocytosis. At the site pointed to by an *arrow*, one bacterium has already been ingested, while another is just starting to enter the phagocytic cup. The first bacterium has been internalized and is fully surrounded by Akt-PH-GFP. The *arrow* points to edge of the membrane where the second bacterium has begun to undergo phagocytosis. The *inset*, *bottom right*, shows a dual phase and fluorescent image of the same bacteria. The phase image shows the extracellular segment of the second bacterium not seen in the fluorescence image. *Bar* = 10 μm. *C*, time 20–40 min after addition of *Listeria* to a culture dish containing cells transfected with PLCδ-PH-GFP. The images are indistinguishable from Akt-PH-GFP. Two bacteria have been ingested and are outlined by the probe. The *arrow* points to the edge of the membrane where the third bacterium is undergoing phagocytosis. The *inset*, *upper right*, shows a phase image, and the *arrow* points to the same location as the fluorescence image.

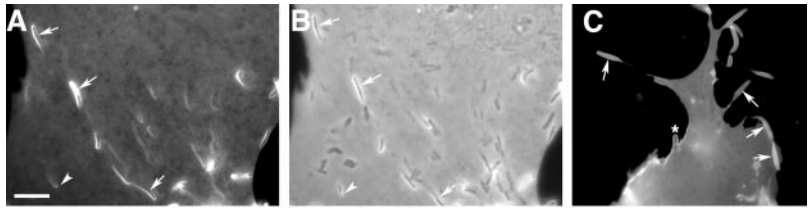

FIG. 2. **Localization of PLCδ-PH-GFP in PtK2 cells 4–5 h after initiation of *Listeria* infection.** *A*, fluorescence image showing a cell expressing PLCδ-PH-GFP 4 h after initiation of *Listeria* infection. At this time bacteria are actively moving through the cytoplasm by actin-based motility. *Arrows* point to the junctions between the phase-dense tails and the motile bacteria. The *arrowhead* points to a motile bacterium that has concentrated PLCδ-PH-GFP at its front, prior to attracting the probe to its tail. *B*, phase contrast combined with the fluorescence image captured 30 s after the image shown in *A*. Note that 45% (24/53) of the intracellular bacteria identified by phase microscopy attracted the fluorescent probe. *Bar* = 10 μm. *C*, fluorescence image of cells expressing PLCδ-PH-GFP 5 h after the initiation of infection. Most of the bacteria have reached the periphery of the cell and formed filopodia (*arrows*). One bacterium can be seen in the early stage of filopod formation (*asterisk*) (see video supplement).

cytoplasm by actin-based motility (Fig. 5, *A* and *C*). Mutant Akt- and PLCδ-PH-GFP probes that have low affinity for phosphoinositides *in vitro* (see "Experimental Procedures") were distributed diffusely throughout the cytoplasm of the cell and failed to localize to the bacteria, indicating that our findings represented specific interactions (data not shown).

To determine whether the two PH domain probes were localizing to the same sites in *Listeria* infected PtK2 cells, cells were simultaneously transfected with PLCδ-PH-GFP and Akt-PH-mRFP and then infected with *Listeria*. As shown in Fig. 3, after 4 h of infection, both probes localized to the surface of the bacteria and to the actin-rich tails. In multiple experiments no consistent difference between the localization of the two probes was detected.

Our combination of phase and fluorescence images suggested that the two PH domains localized to both the bacteria and the actin tails. To compare the distribution of the Akt-PH domain and actin simultaneously, we transfected MDCK cells with both GFP-actin and Akt-PH-mRFP, followed by infection with *Listeria*. Four hours after initiation of infection, distinct differences in the localization of GFP-actin and Akt-PH-mRFP were observed. Although Akt-PH-mRFP concentrated along the surface of the bacterium and along the actin-rich tail, GFP-actin concentrated only at the back of the motile bacteria in tails, as observed previously (6) (Fig. 4).

Effects of Reducing Phosphoinositide Levels on Listeria Intracellular Movement and Filopod Formation—Akt-PH-GFP localization in *Listeria*-infected cells was next examined after treatment with the PI 3-kinase inhibitor, LY294002. At 4–6 h after the initiation of infection PtK2 cells containing motile bacteria-concentrating Akt-PH-GFP were treated with a final concentration of 50 μM LY294002. This concentration has been shown to specifically inhibit PI 3-kinase activity and to quickly block PtdIns(3,4,5)P_3 production in cells (17). Within 15 min of LY294002 exposure, Akt-PH-GFP completely dissociated from the bacteria and filament tails and homogeneously filled the cytoplasm (compare *A* and *B* in Fig. 5). When LY294002 was washed out by exchanging the media with buffer 3 times, Akt-PH-GFP re-concentrated around the bacteria and in the actin tails within 15 min (Fig. 5*C*). Treatment with wortmannin (100 nM final concentration) also dissociated Akt-PH-GFP from the bacterial surface and actin tails (data not shown). Addition of the same concentrations of LY294002 or wortmannin to tissue culture dishes of infected cells containing PLCδ-PH-GFP failed to dissociate this GFP construct from the bacteria or actin tails (data not shown).

Addition of LY294002 at the time the bacteria were actively migrating through the cell by actin-based motility slowed their velocity by more than 60% (0.070 ± 0.002 μm/s pretreatment *versus* 0.024 ± 0.001 μm/s post-treatment, S.E., $n = 98$, $p < 0.0001$, Fig. 6*A*). The inhibition was reversible, and within 15–20 min of removing LY294002, bacterial velocities had returned to control values (0.065 ± 0.002 μm/s, $n = 98$). A slowing of bacterial actin-based motility was also observed after treatment with wortmannin (final concentration 100 nM) (pretreatment velocity 0.083 ± 0.002, S.E., $n = 357$ *versus* post-treatment 0.050 ± 0.002, S.E., $n = 206$, $p < 0.001$) (Fig. 6*A*). The effects of another, less specific PtdIns kinase inhibitor, quercetin, were also examined. This bioflavinoid inhibits PtdIns 4-kinase activity and also caused a significant slowing of *Listeria* intracellular speed (pretreatment mean velocity 0.072 ± 0.003 μm/s, S.E., $n = 104$ *versus* 0.030 ± 0.001, S.E., $n = 196$ post-treatment mean velocity, $p < 0.0001$). However, the degree of inhibition was no greater than that of LY294002

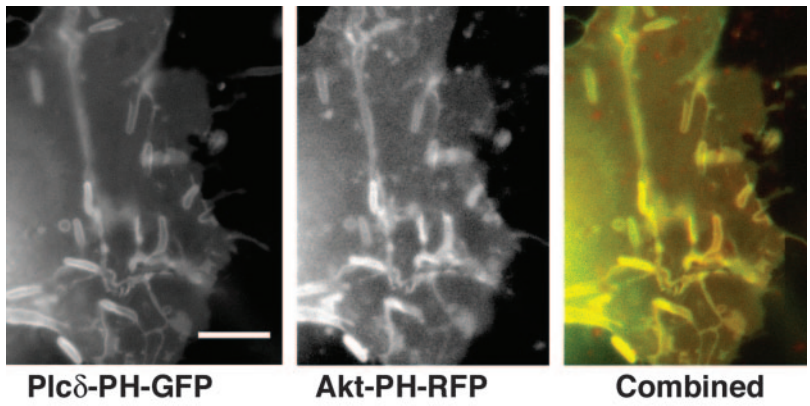

FIG. 3. **Simultaneous presence of PtdIns(4,5)P_2 and PtdIns(3,4,5)P_2 on the surface of *L. monocytogenes* in PtK2 cells.** PtK2 cells were transfected with both PLCδ-PH-GFP and Akt-PH-mRFP for 24 h and infected with *Listeria* for 4 h. PLCδ-PH-GFP (*left panel*, *green channel*) and Akt-PH-mRFP (*middle panel*, *red channel*) both in gray scale show almost identical localization around the moving bacteria and the actin tails. The *right panel* shows an overlay of the two images. *Bar* = 10 μm.

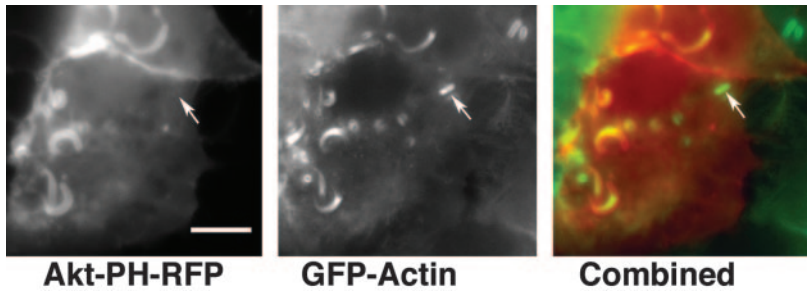

FIG. 4. **Localization of Akt-PH-mRFP and GFP-actin in *Listeria*-infected MDCK cells.** Cells were transfected with both GFP-actin and Akt-PH-mRFP and examined 4 h after initiation of the *Listeria* infection. The *left-hand panel* shows the Akt-PH-mRFP (*red channel*), and the *middle panel* shows GFP-actin (*green channel*), both in gray scale, and the *right-hand color panel* shows a combination of the two images. Note that the two probes co-localize only in the actin-rich tails. Unlike actin, Akt-PH-mRFP fully surrounds the motile bacteria. The one stationary bacterium in the *upper right quadrant* (*arrow*) is *green*, indicating that it has induced actin filament formation around it but has not yet attracted Akt-PH-GFP. *Bar* = 10 μm.

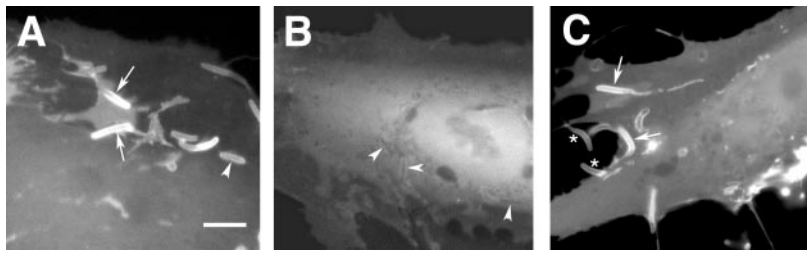

FIG. 5. **The effect of the PI 3-kinase inhibitor, LY294002, on the distribution of the Akt-PH-GFP in PtK2 cells infected with *L. monocytogenes*.** PtK2 cells were transfected with the Akt-PH-GFP and infected with *Listeria* for 4 h. *A*, motile bacteria attract the Akt-PH domain around their bodies and the actin tails as shown in previous figures. The *arrows* point to the interface between the motile bacteria and their actin tails. The *arrowhead* points to a stationary bacterium fully surrounded by the probe. *Bar* = 10 μm. *B*, treatment with LY294002 (50 μM) for 15 min eliminates Akt-PH domain binding. The bacteria are still visible against the cytoplasmic fluorescence (*arrowheads*). *C*, within 30 min of removal of LY294002, Akt-PH-GFP has again concentrated around the bacteria and the actin tails. *Arrows* point to the junction between the bacteria and the actin tails. Two filopodia are each labeled with an *asterisk*.

(Fig. 6*A*). These results prompted us to examine the effects of LY294002 on *Listeria* actin-based motility in a cell-free system, bovine brain extract. Unlike intact cells, the same final concentration of the inhibitor caused no slowing of *Listeria* motility as compared with controls. The velocities of both control and LY294002-treated extracts were approximately one-tenth of those observed in intact cells (controls: 0.0036 ± 0.0002 μm/s, S.E., n = 73 *versus* LY294002: 0.0048 ± 0.003 μm/s, n = 57) (Fig. 6*A*).

To explore the effects of PI 3-kinase inhibition at earlier stages of *Listeria*-induced actin assembly, PtK2 cells were treated with LY294002 1–2 h after the initiation of infection. By this time bacteria have escaped into the cytoplasm and induced the symmetric formation of actin filaments on their surface (sometimes called halos) but have not begun to move or form polar actin filament tails (6). Within 1 h of LY294002 treatment a marked reduction in the percentage of intracellular bacteria surrounded by actin filaments was observed. As assessed by simultaneous phase and rhodamine-phalloidin staining, 5% (20/383) of the bacteria in LY294002-treated cells formed halos, as compared with 68% (569/832) in control cells ($p < 0.0001$). At later time points, bacteria in control cells began to actively move in the cytoplasm. As shown in Fig. 6, *B* and *C*, by 4 h after the initiation of infection 24% (40/167) of intracellular bacteria were actively moving through the cytoplasm and 27% (46/167) had already reached the peripheral membrane and formed filopodia. Therefore, the combined percentage of motile intracellular bacteria was 51% in control cells. At the same time point in LY294002-treated cells only 0.5% (1/211) of intracellular bacteria were moving, and only 7.5% had formed filopodia (16/211), resulting in a total

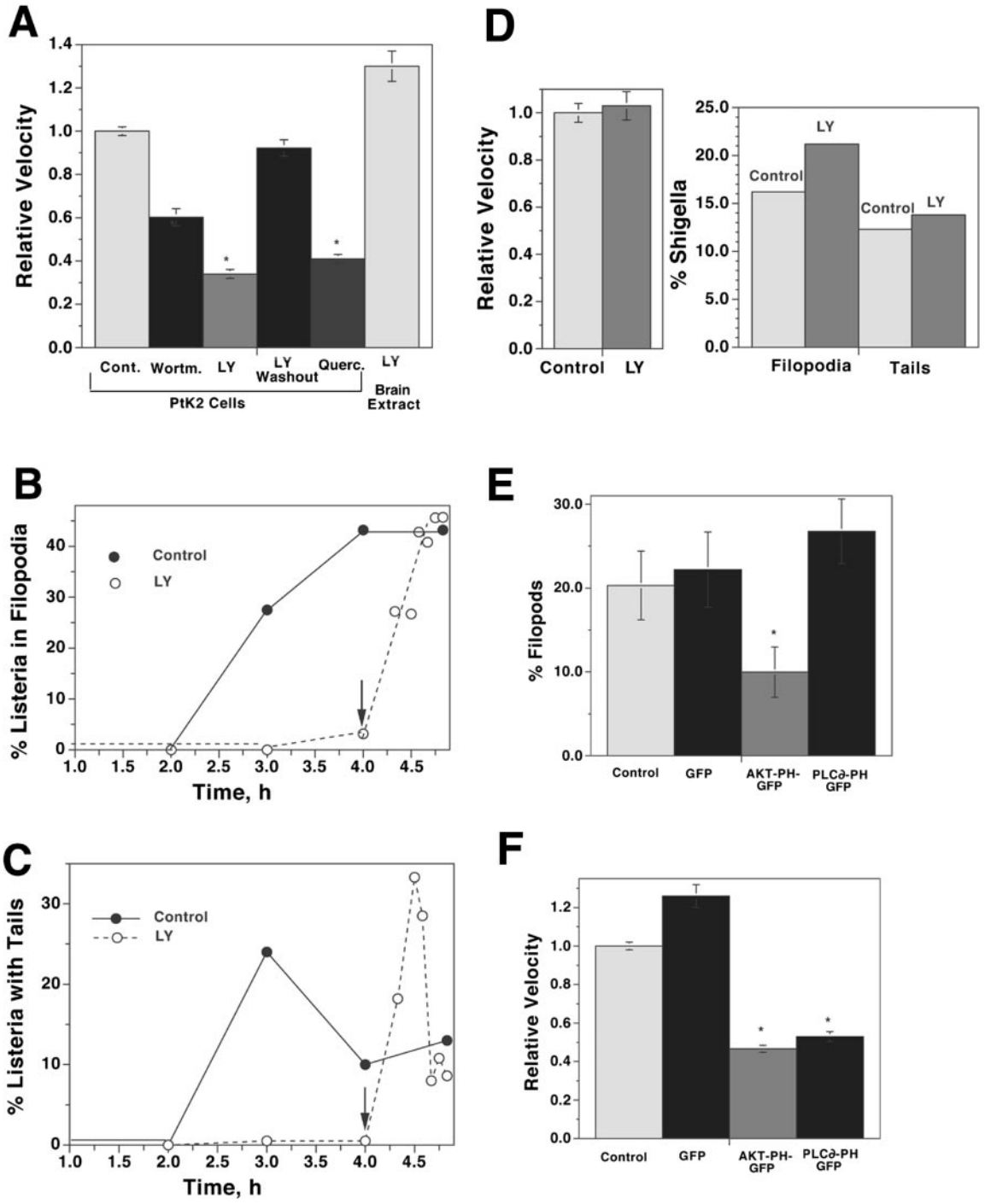

FIG. 6. **Effects of lipid kinase inhibitors and expression of Akt-PH-GFP and PLCδ-PH-GFP on intracellular actin-based movement of *L. monocytogenes*.** *A*, the *bar graph* shows the effects of LY294002 (50 μM), wortmannin (100 nM), and quercetin (50 μM) on *Listeria* actin-based velocity in PtK2 cells, as well as the effects of LY294002 on *Listeria* motility in brain extract. Inhibitors were added 4 h after the initiation of *Listeria* infection in PtK2 cells or simultaneously with the bacteria in the brain extract experiments. Because of the variability in velocities from cell preparation to preparation, the mean velocities of motile bacteria before addition of the inhibitor were given a value of 1.0, and the velocities of treated cells were expressed relative to these respective control values. *Error bars* represent the S.E. of $n = 98–357$ (see results for actual velocities). *B*, line graph showing the changes in the percentage of bacteria forming filopodia over time after the initiation of infection. *Filled circles*, control cells (untreated); *open circles*, LY294002-treated cells. The *arrow* marks the time point when the inhibitor was washed out. *C*, line graph showing the changes in the percentage of intracellular bacteria forming actin tails, indicating active movement within the cytoplasm. *Arrow* marks the time point when LY294002 was washed out. *Filled circles*, control cells; *open circles*, LY294002-treated cells. *D*, *left*, bar graph comparing the relative velocities of *Shigella* in untreated PtK2 cells (control, *light gray*) and cells treated with LY294002 (50 μM, *LY*, *dark gray bar*). *Error bars* represent the S.E. of $n = 326–424$. See text for actual velocities. *D*, *right*, bar graph comparing the percentage of intracellular *Shigella* that formed filopodia and actin-rich tails in the absence (control, *light gray bars*) or presence of 50 μM LY294002 (*LY*, *dark gray bars*), $n = 716$ bacteria for control and 571 bacteria for LY294002-treated cells. *E*, the percentage of intracellular *Listeria* forming filopodia in infected PtK2 cells transfected with the different GFP-PH constructs were compared with control cells. Akt-PH-GFP, but not PLCδ-PH, inhibited filopod formation. *Error bars* represent the S.E. of $n = 20–30$ cells. The *asterisk* indicates a statistically significant difference from controls, $p = 0.013$. *F*, velocities of *Listeria* in PtK2 cells transfected with different GFP-PH constructs. Both the Akt-PH-GFP and PLCδ-PH-GFP significantly decreased the mean velocities compared with untransfected or GFP-transfected PtK2 cells. *Error bars* represent the S.E. of $n = 200–500$. *Asterisks* indicate statistically significant differences from controls, $p < 0.0001$.

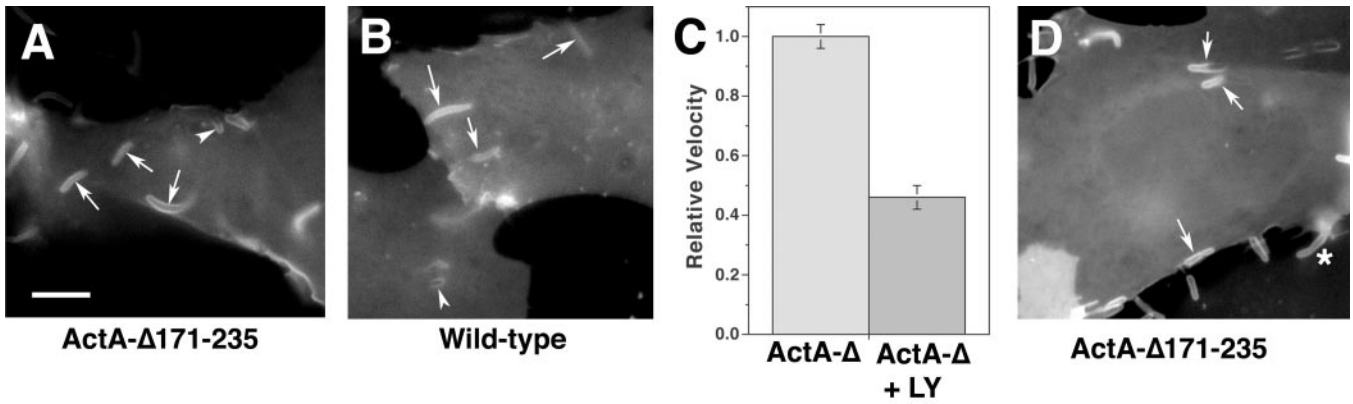

FIG. 7. **Effects of deleting the putative phosphoinositide binding site on *Listeria* ActA on its ability to attract Akt-PH-GFP and PLCδ-PH-GFP and respond to PI 3-kinase inhibitors.** *A*, localization of Akt-PH-GFP to the bacterial surface and actin tails of *Listeria* DP-L3982 (ActA-$\Delta_{171-235}$) in PtK2 cells 4 h after the initiation of infection. *Arrows* point to the junction between the bacteria and actin tail in all three fluorescence images (*A*, *B*, and *D*), and *arrowheads* point to bacteria that have localized the probe to their front. *B*, localization of Akt-PH-GFP to the surface of wild-type *Listeria* 10403S strain 4 h after infection. No significant difference in the localization of either Akt-PH-GFP or PLCδ-PH-GFP was detected comparing wild type to the ActA mutant bacteria. *Bar* = 10 μm. *C*, inhibitory effect of LY294002 on the mean velocity of *Listeria* DP3982 (ActA-$\Delta_{171-235}$) in PtK2 cells. *Error bars* represent the S.E. of $n = 80-350$ measurements. The reduction in velocity was highly significant, $p < 0.0001$. *D*, localization of PLCδ-PH-GFP to the bacterial surface and actin tails of *Listeria* DP-L3982 (ActA-$\Delta_{171-235}$) in PtK2 cells 4 h after initiation of infection. *Asterisk* marks a filopod.

percentage of motile bacteria of only 8%. These differences were highly significant ($p < 0.0001$). At 5 h similar differences were observed between bacteria in control and treated cells (Fig. 6, *B* and *C*). When LY294002 was washed out of the tissue culture dishes, a complete reversal of inhibition was observed. Within 25 min of removal of the LY294002, 33% of intracellular bacteria were migrating through the cytoplasm, and 27% had formed filopodia (total percentage of motile bacteria = 60%) (Fig. 6, *B* and *C*). A linear rise in the percentage of intracellular bacteria forming filopodia was observed over the first 50 min after washout (Fig. 6*B*). Rhodamine phalloidin staining showed that in the presence of LY294002, the F-actin content of bacterial actin tails was significantly lower than that observed in control cells, the mean relative fluorescence intensity of actin tails in treated cells (mean relative intensity 8.2 ± 1.0, $n = 45$) being less than one-third of mean intensity of actin tails in untreated cells (mean relative intensity 27.7 ± 1.2, $n = 62$, $p < 0.0001$).

The effects of LY294002 were also examined on another intracellular pathogen known to move by actin-based motility within the cytoplasm of cells, *S. flexneri*. PtK2 cells were infected with *Shigella* and the inhibitor (final concentration of LY294002 = 50 μM) added at the time of infection or 1 h after the initiation of infection. Addition of LY294002 at either time point had no significant effect on the velocity of *Shigella* actin-based motility (Fig. 6*D*, left) (mean velocity of untreated cells, 0.048 ± 0.002 μm/s, S.E., $n = 434$ *versus* LY294002-treated cells, 0.049 ± 0.003 μm/s, $n = 326$), and this treatment failed to reduce the percentage of bacteria forming filopodia or forming actin-rich tails (Fig. 6*D*, right). Consistent with these findings, *Shigella* failed to attract Akt-PH-GFP or PLCδ-PH-GFP to its surface or to its actin tails in five separate experiments (data not shown).

Because PLCδ-PH and Akt-PH bind specific phosphoinositides with relatively high affinity, these probes would be expected to reduce the availability of these phosphoinositides for the enhancement of *Listeria* actin-based motility. To assess the functional consequences of the sequestration of these lipids, we examined the percentage of intracellular bacteria that formed filopodia in transfected *versus* control cells at 4–5 h after *Listeria* infection. As shown in Fig. 6*E*, Akt-PH-GFP transfection significantly reduced filopod formation as compared with GFP alone, and PLCδ-PH-GFP showed no inhibitory effect on this parameter. However, analysis of the intracellular speeds of *Listeria* revealed an ~50% reduction in both Akt-PH-GFP and PLCδ-PH-GFP transfected cells as compared with control or GFP transfected cells (Fig. 6*F*).

Comparison of Wild-type to L. monocytogenes ActA Mutants Lacking the Phosphoinositide Binding Site—The surface protein ActA on wild-type *Listeria* contains a putative binding site for D3 and D4 phosphoinositides. Therefore, we explored the possibility that this binding site was responsible for the localization of the two GFP-PH domains to the bacterial surface and to actin tails of intracellular motile *Listeria*. Two *Listeria* mutants containing an ActA surface protein in which the phosphoinositide binding site had been deleted, *Listeria* ActA-$\Delta_{171-235}$ called DP-L3982 (12) and *Listeria* ActA-$\Delta_{158-231}$ called bacteria 1368 (10), were tested. As shown in Fig. 7*A*, the DP-L3982 mutant strain was able to concentrate Akt-PH-GFP on its surface and in the actin tails, and the pattern and extent of localization was indistinguishable from that of wild-type bacteria (compare *A* and *B* of Fig. 7). Identical results were observed with *Listeria* mutant strain 1398 (data not shown). Similarly to wild-type *Listeria*, treatment with LY294002 (final concentration 50 μM) dissociated the probe from the mutant DP-L3982 (data not shown) and slowed intracellular actin-based motility (Fig. 7*C*). Both mutant bacteria were also able to attract PLCδ-PH-GFP and concentrate this probe in the identical regions observed for Akt-PH-GFP (Fig. 7*D*).

Localization of GFP-Akt-PH following Latrunculin Treatment—To determine whether the localization of the PH domains was a consequence of actin polymerization, the effects of treating cells with the actin monomer sequestering agent latrunculin on Akt-PH-GFP localization were examined. As shown in Fig. 8, a concentration of latrunculin that depolymerized all phase-dense *Listeria* actin tails had minimal effects on localization of the probe around the bacterium. However latrunculin treatment did alter the morphology of the probe in the region of the actin filament tail. The Akt-PH-GFP localization to the tail region became irregular (Fig. 8, *arrow*, 10 min after initiation of latrunculin treatment), and eventually the tail collapsed (Fig. 8, *arrow*, 20-min image).

DISCUSSION

There has been great interest in the localization of phosphoinositides during cell motility, and extensive evidence documents that the D3 and D4 phosphoinositides concentrate in areas where new actin structures are forming. However the exact functional roles of these phosphoinositides during actin-based motility remains to be determined. During phagocytosis,

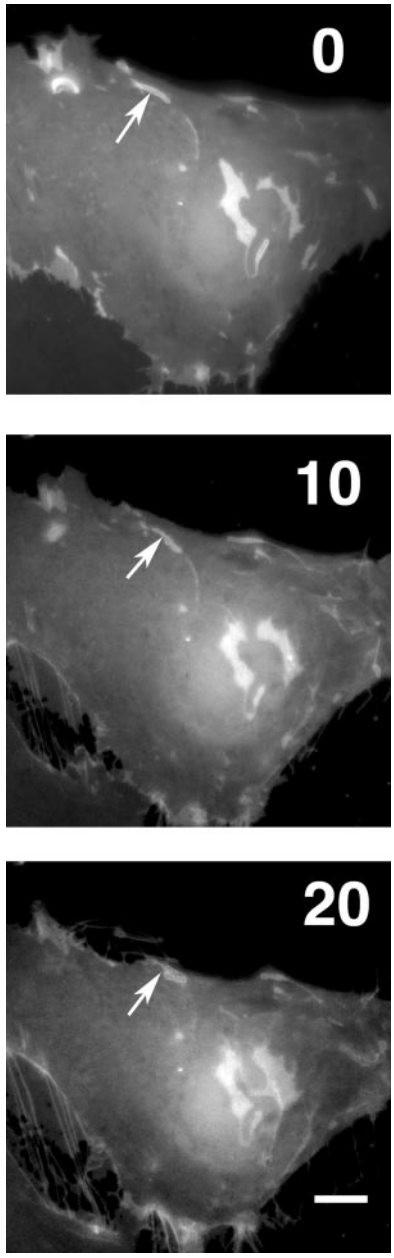

FIG. 8. **The effect of latrunculin treatment on Akt-PH-GFP localization in PtK2 cells infected with *Listeria* for 4 h.** Pictures were taken before and 10 and 20 min after the addition of 2 μM latrunculin (represented by the *numbers* in the *upper right*). The *arrow* points to the junction between the bacterium and phase-dense tail determined by simultaneous phase microscopy. Note that the movement of the bacteria is inhibited by latrunculin, and the localization of the Akt-PH-GFP to the actin tail, but not to the body of the bacteria, is inhibited. *Bar* = 10 μm.

PtdIns(4,5)P_2 accumulates in the early extending pseudopods and then quickly disappears whereas PtdIns(3,4,5)P_3 concentrates at the base of the phagocytic cup (18). These observations are consistent with PtdIns(4,5)P_2 serving as the substrate for the production of PtdIns(3,4,5)$_3$ in response to a phagocytic stimulus. PtdIns(4,5)P_2 also serves as a substrate for the PLC-mediated production of diacylglycerol which stimulates protein kinase C (19) and inositol 1,4,5-triphosphate, which releases intracellular stores of Ca^{2+} (20). In addition to serving as a substrate, PtdIns(4,5)P_2 could directly affect the function of other proteins within the cell, and the functions of a number of proteins related to actin polymerization have been linked to phosphoinositides, including the uncapping of actin filaments, sequestration of profilin, and the stimulation of Arp2/3 nucleation of actin assembly via N-WASP or WASP (2). However, the role of PtdIns(3,4,5)P_3 in actin-based motility is less well understood. It has been clearly linked to actin polymerization during chemotaxis (21), and it may recruit myosin X to the site of phagocytosis (22). The effects of the inositides are probably also mediated through activation of small GTP-binding proteins of the Rho family via recruitment of guanine nucleotide exchange factors (23).

Unlike phagocytosis and chemotaxis, which result in stimulation of the Rho family GTPases Rac and Cdc42 (21), intracellular *Listeria* bypasses these signal transduction pathways. Its ActA protein directly stimulates Arp2/3 to nucleate actin assembly and is not believed to require activation of small GTP-binding proteins (24). Recent work in our laboratory also indicates that changes in intracellular calcium do not affect the speed of intracellular *Listeria* (25). Therefore, many of the classically proposed functions of PtdIns(4,5)P_2 and PtdIns(3,4,5)P_3 do not apply to *Listeria*.

In the simple reconstituted system consisting of Arp2/3 complex, ADF/cofilin, CapZ, and actin, phosphoinositides are not required for *Listeria* actin-based motility (26). However, the purified system is far more permissive and only supports velocities that are approximately one-tenth of those observed in the intact cell. Although this simplified system has proved very helpful in clarifying the minimal components required to initiate actin-based motility, such extracts do not fully recapitulate the events taking place in the cell. The viscosity of the cytoplasm, as well as the compartmentalization of many components, provide a far more challenging environment for the initiation and maintenance of actin-based motility. Also, the discovery of a putative phosphoinositide binding site on the *Listeria* surface protein ActA encouraged us to explore the possibility that *Listeria* might utilize these lipid products to stimulate actin filament assembly in the intact cell. First, as noted in macrophages during ingestion of IgG opsonized particles (16, 18), both PtdIns(4,5)P_2 and PtdIns(3,4,5)P_3 accumulated in the region where *Listeria* was being phagocytosed (Fig. 1). However, these lipids remained associated with the engulfed bacteria only for a short period of time (1–5 min), being followed by a period of 3–4 h during which the presence of phosphoinositides at the bacterial surface was not readily detected. When the bacteria began to move and form actin filament tails, both PtdIns(4,5)P_2 and PtdIns(3,4,5)P_3 started to accumulate around the bacteria. We originally predicted that the phosphoinositides would be attracted to the back of the moving *Listeria* to uncap actin filaments in the polymerization zone and thereby stimulate polar actin filament assembly. However, we were surprised to find that both PLCδ-PH-GFP and Akt-PH-GFP first localize to the front of motile bacteria at regions of the bacterial surface that do not induce the formation of actin filaments (Fig. 2 and Fig. 2 video supplement). The PH domain probes subsequently concentrate along the side of the bacteria and in the actin filament tails. Furthermore, depolymerization of the actin tails by addition of latrunculin did not dissociate these probes from the surface of the bacteria, only from the actin filament tails (Fig. 8). These findings suggest that PtdIns(4,5)P_2 and PtdIns(3,4,5)P_3 are likely to serve multiple roles in addition to modifying the functions of actin-binding proteins in the polymerization zone.

PLCδ-PH-GFP and Akt-PH-GFP were concentrated around 10–60% of motile bacteria. Bacteria with the highest likelihood of concentrating the two PH-GFP probes were located near the peripheral membrane and produced phase-dense tails (caused by light refraction by actin filaments). This observation suggests that the bacteria might attract phosphoinositides from the inner leaflet of the plasma membrane. It is also possible that higher concentrations of phosphoinositides are required to move through this region of the cell where high concentrations

of filamentous actin are commonly found. We frequently observed that within 1–2 min after becoming surrounded by the PH-GFP probes, the bacterium moved out of the cell forming a filopod. This observation may suggest that recruitment of PtdIns(4,5)P_2 and PtdIns(3,4,5)P_3 is required for efficient production of filopodia, and the production of these structures is required for efficient spread of *Listeria* from cell to cell.

How does *Listeria* attract PtdIns(4,5)P_2 and stimulate production of PtdIns(3,4,5)P_3? The finding of a phosphoinositide binding site at amino acids 184–202 on ActA suggested that this binding site could account for the ability of the bacterium to attract these phosphoinositides (9). It was proposed that the binding of PtdIns(4,5)P_2 by ActA might serve to deliver this phosphoinositide to the actin polymerization zone of *Listeria* and uncap actin filaments. However, *in vitro* experiments subsequently demonstrated that sequestration of PtdIns(4,5)P_2 by ActA actually inhibited the ability of the phosphoinositide to uncap actin filaments (10). Furthermore, deletion of the inositide binding site was reported only to minimally affect intracellular actin-based motility and not to alter the ability of *Listeria* to spread from cell to cell (10, 12). Consistent with these findings, we found that the loss of the putative inositide binding domain of ActA did not affect localization of PtdIns(4,5)P_2 and PtdIns(3,4,5)P_3 to the surface of intracellular *Listeria* and their actin tails (Fig. 7). The ActA-$\Delta_{171–235}$ and wild-type bacteria also demonstrated comparable sensitivities to the PI 3-kinase inhibitor LY294002, further supporting this conclusion and suggesting that either another region of ActA or another bacterial surface protein may be responsible for concentrating these phosphoinositides.

The finding that the PI 3-kinase inhibitor LY294002 causes near complete inhibition of *Listeria* actin-based motility indicates that PtdIns(3,4,5)P_3 plays a critical role in *Listeria* actin-based motility within the cell. Addition of this inhibitor results in rapid dissociation of Akt-PH-GFP from the bacterial surface and in motile bacteria results in a slowing of bacterial intracellular speed. Reduction of available PtdIns(4,5)P_2 or PtdIns(3,4,5)P_3 also results in the slowing of bacterial speed, and the data together suggest that PtdIns(4,5)P_2 is recruited and converted to PtdIns(3,4,5)P_3 on the bacterial surface (Figs. 5 and 6). Maximum inhibition of LY294002 is achieved when the inhibitor is added 1–2 h after the initiation of infection, at the time when *Listeria* is growing in the cytoplasm and is inducing actin filaments that fully surround the bacterium.

Our observation that *Shigella* actin-based motility is not impaired by LY294002, combined with our finding that *Shigella* does not attract Akt-PH-GFP to its surface, indicates that PtdIns(3,4,5)P_3 is not required for all forms of intracellular bacterial actin-based motility. *Shigella*, unlike *Listeria*, requires N-WASP to activate the Arp2/3 complex and uses the surface protein IcsA, a protein that is structurally unrelated to ActA. The profound inhibition of *Listeria*-induced actin assembly caused by the blockade of PI 3-kinase activity indicates that continued production of PtdIns(3,4,5)P_3 is required for ActA (or another protein or proteins) to function in the host cell cytoplasm and raises the possibility that PtdIns(3,4,5)P_3 may be required for a post-translational modification of ActA or a partner protein responsible for the induction of actin filament formation. PtdIns(3,4,5)P_3 may target a kinase or other modifying enzyme to the bacterial surface to accomplish this task. It is also possible that this phosphoinositide directly modifies the activity of one or more actin-regulatory proteins to initiate actin filament formation. We are presently exploring these possibilities.

In conclusion, the present data support a critical role for PI 3-kinase activity in *Listeria* actin-based motility and for the first time demonstrate that *Listeria* is capable of concentrating both PtdIns(4,5)P_2 and PtdIns(3,4,5)P_3 on its surface *in vivo*. Binding of these phospholipids does not require the putative ActA lipid binding site. Our findings suggest that PtdIns(3,4,5)P_3 and its precursor PtdIns(4,5)P_2 are critical mediators of *Listeria* intracellular actin-based motility. Furthermore our results are most consistent with PtdIns(3,4,5)P_3 serving as a regulator of ActA activity in the intact cell. The simplicity of the *Listeria* model system has provided an excellent vehicle for clarifying the functional role of phosphoinositides in actin filament assembly, and this model system promises to allow further dissection of this important signal transduction pathway.

Acknowledgments—We thank Dr. Pascale Cossart of the Institute Pasteur, Paris, France and Dr. Daniel Portnoy of the University of California, Berkeley, for their ActA-mutant *Listeria* strains and Dr. Beat Imhof, University of Geneva, Geneva, Switzerland for providing enhanced GFP-actin MDCK cells.

REFERENCES

1. Czech, M. P. (2000) *Cell* **100,** 603–606
2. Yin, H. L., and Janmey, P. A. (2003) *Annu. Rev. Physiol.* **65,** 761–789
3. Postma, M., Bosgraaf, L., Loovers, H. M., and Van Haastert, P. J. (2004) *EMBO Rep.* **5,** 35–40
4. Pizarro-Cerda, J., Sousa, S., and Cossart, P. (2004) *C. R. Biol.* **327,** 115–123
5. Portnoy, D. A., Jacks, P. S., and Hinrichs, D. J. (1988) *J. Exp. Med.* **167,** 1459–1471
6. Dabiri, G. A., Sanger, J. M., Portnoy, D. A., and Southwick, F. S. (1990) *Proc. Natl. Acad. Sci. U. S. A.* **87,** 6068–6072
7. Sanger, J. M., Sanger, J. W., and Southwick, F. S. (1992) *Infect. Immun.* **60,** 3609–3619
8. Cossart, P. (2000) *Cell Microbiol.* **2,** 195–205
9. Cicchetti, G., Maurer, P., Wagener, P., and Kocks, C. (1999) *J. Biol. Chem.* **274,** 33616–33626
10. Steffen, P., Schafer, D. A., David, V., Gouin, E., Cooper, J. A., and Cossart, P. (2000) *Cell Motil. Cytoskeleton* **45,** 58–66
11. Lemmon, M. A., Ferguson, K. M., O'Brien, R., Sigler, P. B., and Schlessinger, J. (1995) *Proc. Natl. Acad. Sci. U. S. A.* **92,** 10472–10476
12. Skoble, J., Portnoy, D. A., and Welch, M. D. (2000) *J. Cell Biol.* **150,** 527–538
13. Zeile, W. L., Purich, D. L., and Southwick, F. S. (1996) *J. Cell Biol.* **133,** 49–59
14. Varnai, P., and Balla, T. (1998) *J. Cell Biol.* **143,** 501–510
15. May, R. C., Hall, M. E., Higgs, H. N., Pollard, T. D., Chakraborty, T., Wehland, J., Machesky, L. M., and Sechi, A. S. (1999) *Curr. Biol.* **9,** 759–762
16. Botelho, R. J., Scott, C. C., and Grinstein, S. (2004) *Curr. Top. Microbiol. Immunol.* **282,** 1–30
17. Vlahos, C. J., Matter, W. F., Hui, K. Y., and Brown, R. F. (1994) *J. Biol. Chem.* **269,** 5241–5248
18. Botelho, R. J., Teruel, M., Dierckman, R., Anderson, R., Wells, A., York, J. D., Meyer, T., and Grinstein, S. (2000) *J. Cell Biol.* **151,** 1353–1368
19. Dillon, S. B., Murray, J. J., Uhing, R. J., and Snyderman, R. (1987) *J. Cell. Biochem.* **35,** 345–359
20. Berridge, M. J., Lipp, P., and Bootman, M. D. (2000) *Nat. Rev. Mol. Cell. Biol.* **1,** 11–21
21. Srinivasan, S., Wang, F., Glavas, S., Ott, A., Hofmann, F., Aktories, K., Kalman, D., and Bourne, H. R. (2003) *J. Cell Biol.* **160,** 375–385
22. Hilpela, P., Vartiainen, M. K., and Lappalainen, P. (2004) *Curr. Top. Microbiol. Immunol.* **282,** 117–163
23. Welch, H. C., Coadwell, W. J., Stephens, L. R., and Hawkins, P. T. (2003) *FEBS Lett.* **546,** 93–97
24. Moreau, V., and Way, M. (1998) *FEBS Lett.* **427,** 353–356
25. Larson, L., Arnaudeau, S., Gibson, B., Li, W., Krause, R., Hao, B., Bamburg, J. R., Lew, D. P., Dermaurex, N., and Southwick, F. (2005) *Proc. Natl. Acad. Sci. U. S. A.*, in press
26. Loisel, T. P., Boujemaa, R., Pantaloni, D., and Carlier, M. F. (1999) *Nature* **401,** 613–616